Production of PEGylated nanocapsules through solvent displacement in confined impinging jet mixers

Production of PEGylated nanocapsules through solvent-displacement in confined impinging jets mixers

Ilaria Valente[1*], Barbara Stella[2], Daniele L. Marchisio[1], Franco Dosio[2], Antonello A. Barresi[1]

[1]Politecnico di Torino, Dipartimento di Scienza dei Materiali e Ingegneria Chimica, Corso Duca degli Abruzzi 24, 10129 Torino, Italy;

[2]Università degli Studi di Torino, Dipartimento di Scienza e Tecnologia del Farmaco, via Pietro Giuria 9, 10125 Torino, Italy

ABSTRACT:

The growth of importance of nanocapsules (and other particulate systems) in different fields requires fast and reproducible methods for their production. Confined impinging jet mixers were successfully used for the production of nanospheres and are now tested for the first time for the production of nanocapsules. This work focuses on the understanding of formation mechanisms and on the quantification of the effect of the most important operating parameters involved in their production. Solvent displacement is employed here for the assembly of the nanocapsules by using a PEGylated derivative of cyanoacrylate as copolymer. A comparison with nanospheres obtained under the same operating conditions is also reported. Results show that the oil-to-copolymer mass ratio (MR) is the main factor affecting the final size distribution and that small nanocapsules are obtained only at low oil-to-copolymer MR. The effect of mixing is significant, proving that mixing of solvent and antisolvent also affects the final size distribution; this depends mainly on the inlet jet velocity, but the size of the mixer is also important. The Reynolds number may be useful to take this into account for geometrically similar systems. Quenching by dilution allows to stabilize the nanocapsules, evidencing the role of aggregation and ripening

Keywords:

Nanocapsules, nanospheres, copolymer nanoparticles, confined impinging jets mixer, nano-flash precipitation, solvent-displacement

(*) corresponding author: Tel: +39-011-5644679, Fax: +39-011-5644699, Email: ilaria.valente@polito.it

INTRODUCTION

In the last years, the pharmaceutical interest in nanotechnology has widen because of the possibilities it offers in releasing drug molecules, enhancing their therapeutic activity, reducing side effects, and increasing the lifetime of the drug *in vivo*. Different nanocarriers have been investigated, namely, liposomes, solid lipid particles, microparticles, and nanoparticles based on synthetic or natural polymers. Polymer nanoparticles include polymeric nanospheres and polymeric nanocapsules. In nanospheres, the drug is incorporated in the polymeric matrix, whereas polymeric nanocapsules have an inner liquid core surrounded by a polymeric layer, so that a large variety of drugs can be dissolved in the inner core, according to their solubility. The drug molecules inside the nanospheres are generally dispersed in the polymer matrix in a sort of solid solution but may also form a solid core coated by the polymer, whereas in nanocapsules they are dissolved in the liquid core; as a consequence, drug release occurs according to different mechanisms in nanospheres and nanocapsules. It depends on biodegradation and bioerosion of the polymer by enzymes and on drug diffusivity through the polymeric matrix, in the case of nanospheres, whereas in nanocapsules it depends also on the partitioning between the media inside and outside the polymeric shell.**1** In comparison to nanospheres, nanocapsules need a lower amount of polymer and can be loaded with larger amounts of drug, depending on the drug solubility in the inner liquid.**2** This work focuses on polymeric nanocapsules for pharmaceutical applications, but nanocapsules find wide use also in the cosmetic and agrochemical fields. The wide growth of their application requires innovative methods for faster production; the use of micromixers is here investigated for the first time.

Polymers from the family of poly(alkyl cyanoacrylates) (PACA) have been extensively used for the preparation of drug carriers. PACA nanoparticles are very common, thanks to their ability to achieve tissue targeting and enhance the intracellular penetration of drugs.**3** The amphiphilic copolymer poly(methoxy polyethylene glycol cyanoacrylate-*co*-hexadecyl cyanoacrylate)**4**, indicated as poly(MePEGCA-*co*-HDCA) in what follows, is used in this work. This kind of copolymer allows to obtain “stealth” nanocapsules, thanks to the polyethylene glycol (PEG) chains. In fact, a limit of standard polymer nanoparticles, without PEG chains, is that *in vivo* opsonins adsorb onto their surface and then nanoparticles can be recognized by macrophages and can be accumulated in liver and spleen. A PEG coating increases their blood lifetime because it creates an aqueous shell around the nanoparticle, which avoids opsonin adsorption and the subsequent macrophage uptake.

Polymer nanocapsules, as well as nanospheres, can be prepared both by polymerization methods**5**,**6**and from preformed polymer, by different mechanisms such as, for example, solvent displacement,**7**emulsion–diffusion,**8** double emulsification,**9** and so on. The different processes and

the characteristics of the nanocapsules produced have been recently compared.**10** In solvent displacement methods (also called interfacial deposition or flash nanoprecipitation), the polymer is prepared in a previous step, resulting in some advantages with respect to interfacial polymerization. In fact, solvent displacement allows to use polymers with controlled molecular weight, avoids the presence of residual monomers in solution, it is simpler and more reproducible, and it is easier to scale-up. Solvent displacement consists of mixing a water-miscible organic phase, containing the polymer, the oil, and generally the drug, with an aqueous phase. The organic phase is referred to as solvent, whereas water is the antisolvent. When the two phases are mixed together, the organic phase diffuses rapidly into the water, where it is soluble and where on the contrary the polymer, the oil, and the drug are insoluble. The rapid diffusion of the solvent in the antisolvent is the driving force in nanocapsules formation, inducing oily drops formation and the interfacial deposition of the polymer around the oily drops.

The overall process being very rapid, it is influenced by mixing and in order to obtain good mixing conditions, special micromixers must be used. Confined impinging jet mixers (CIJMs) provide optimum mixing conditions. Their use in nanosphere formation was extensively studied**11–13** and they were found to be very useful in controlling the final particle size.**14** CIJMs consist of two high velocity linear jets of fluid that collide inside a small chamber, whose size affects the overall mixing rate.

Mixing mechanism and nanoparticle formation in CIJMs, similar to the ones studied in this work, were analyzed in previous papers through computational fluid dynamics (CFD) simulations.**15**,**16** CFD simulations allow to quantify the mixing dynamics of the two inlet streams inside the mixing chamber. Three types of mixing mechanisms are generally present: macromixing at the mixer scale, mesomixing at the scale of the largest turbulent eddies, and micromixing at the molecular scale. Each step controls the next one and can be rate limiting. CIJMs limit the mesomixing time and ensure fast homogenization (i.e., short macromixing time) of the two fluids. Characteristic global mixing times in these equipments were calculated by CFD and are in the order of magnitude of milliseconds.**17**,**18**

In this work, the use of the CIJMs for the production of polymer nanocapsules suitable for pharmaceutical applications is investigated for the first time. As the mechanisms of nanocapsule formation are likely different from those of nanospheres, we are particularly interested in investigating the interplay between mixing and nanocapsules formation, with the precise scope of highlighting similarities and differences. Attention is paid to the control of nanocapsule size distribution. In fact, different applications translate into different requirements. For example, in the case of intravenous administration, nanocapsules have to be smaller than 300 nm. For other

applications, such as cosmetic**19** and food,**20** size limitations are different; therefore, the development of strategies to control the final nanocapsule size turns out to be very useful. Our work aims also at understanding if mixing can be used (also for nanocapsule) as an active parameter to control and tune the final size distribution.

It should be highlighted that no drug has been considered in this work. Although in the case of nanospheres, the absence or the presence of the drug can significantly alter the results (and can modify the particle structure), especially in terms of stability (as shown, for example, for doxorubicin-loaded polymer nanospheres**21**), in the case of nanocapsules, the situation seems to be very different, representing yet another difference between the two systems. In fact, the oil separates from the initial single-phase system through spinodal decomposition; no energetic barrier has to be overcome (as dictated by the Cahn–Hilliard equation) and molecular diffusion is the bottleneck. As the drug is generally hydrophobic and in low concentration (in comparison with the oil), drug molecules will likely move rapidly inside the oily drops. Indeed, a successive study with a drug is required to prove this last point and this simpler oil–polymer system will be used as reference.

THEORETICAL BACKGROUND

The formation of nanocapsules and nanospheres during solvent displacement is a complex process and many theories and interpretations have been presented in the literature. Knowledge of what happens at the molecular level is of primary importance for manipulating and controlling the overall process. Classical precipitation theory explains particle formation in three steps: nucleation, molecular growth, and particle aggregation.**22** Supersaturation is the driving force for particle formation and in solvent displacement processes, it is built up by mixing of the solvent and the antisolvent. As in this work we are interested in both nanospheres and nanocapsules, it is necessary to review and briefly discuss the theory presented in the literature for these two systems.

In the case of nanospheres, the copolymer and organic compound are dissolved in the solvent and when mixed with the antisolvent, particles are formed. Johnson and Prud'homme**23** describe nanosphere formation as the competition of two simultaneous phenomena: nucleation of drug particles and copolymer self-assembly. The two phenomena are characterized by different time scales and in order to allow the copolymer molecules to interact with (and to deposit on) the growing particles, the two time scales have to match one another. Typical operating conditions, used in the production of most of the organic drug particles, are characterized by extremely high

supersaturation, resulting in very small nucleus size, practically instantaneous nucleation, with very little energy barrier. It is also important to compare these time scales with the mixing time scale. It was in fact observed that faster mixing generally results in smaller drug particles with higher functionalization by the copolymer; however, once a certain limit is reached, no significant change in nanoparticle properties is observed. This is probably related to the development of a spatially independent self-similar state caused by the achievement of fully turbulent flow.

In the case of nanocapsules, the inner core of the particle consists instead of a lipophilic liquid (usually oil), which is insoluble in the mixture of solvent and antisolvent. Thus, in nanocapsule formation, two phenomena are involved: oily drop formation and polymer deposition around the oily drop. Oily drop formation takes place through spinodal decomposition (as dictated by the Cahn–Hilliard equation). Therefore, although due to the high supersaturation the nucleation process involved in nanosphere formation generates a very small energy barrier, some differences between nanospheres and nanocapsules, where on the contrary spinodal decomposition occurs spontaneously without any energy barrier, might be observed.

In addition, when solvent and antisolvent are mixed together, the oil dissolved in the solvent separates, resulting in drops which tend to coalesce. This can be prevented (as in the case of nanospheres) by the deposition of the copolymer around the drops; however, in the case of nanocapsules, copolymer reorientation on the interface might play a different role. In any case, also for nanocapsules, mixing efficiency is expected to be fundamental in order to have homogeneous and optimal conditions for the formation of very small drops and an even distribution of copolymer molecules around drops.

Some authors**24**,**25** have acknowledged the important contribution of the Gibbs–Marangoni effect on the formation of nanocapsules, in which the driving force is the difference in the interfacial tension between the solvent and the antisolvent. This effect is not considered in this work because it is important when nanocapsules are produced with the classical method, adding slowly the solvent to the aqueous phase. Using micromixers, such as CIJMs, under very intense turbulent mixing conditions, this effect is expected to be less important.

MATERIALS AND METHODS

The poly(MePEGCA-*co*-HDCA) copolymer was synthesized by condensation of the two monomers (MePEG cyanoacetate and *n*-hexadecyl cyanoacetate) in ethanol and dichloromethane. The ratio

between MePEG cyanoacetate/hexadecyl cyanoacetate was 1:4. The synthesis was carried out under the presence of formaldehyde and dimethylamine, as described in another work,**17** following the procedure of Peracchia et al.,**26** with some minor changes.

The copolymer was characterized in terms of its molecular weight, by using dynamic light scattering (DLS) and by resorting to the Debye theory, by differential scanning calorimetry and by ^{1}H NMR.**17** DLS characterization resulted in a molecular weight of about 4.37 kDa, whereas the two other characterizations confirmed the presence of the two monomers (the lipophilic one, HDCA, and the hydrophilic one, MePEGCA) and their approximate ratio of 1:4.

In all the experiments, Miglyol® 812N (a mixture of capric and caprylic acid) was used as liquid core (courtesy of Sasol Italy S.p.A). The solvent is Acetone Chromasolv (high-performance liquid chromatography grade), purchased by Sigma–Aldrich Italia (Milano). Milli-Q RG system by Millipore® (Billerica, MA, USA) was used to produce the ultrapure water employed in all the experiments.

Nanocapsules and nanospheres were prepared by solvent displacement. In nanocapsule precipitation, the copolymer together with Miglyol® was dissolved in acetone and then mixed with pure water, whereas in nanospheres, only the copolymer was dissolved in the solvent. Apart from this, the two preparations were identical. After mixing with water, the particulate system was immediately formed. As already mentioned, since the process is strongly influenced by mixing, CIJMs were used that ensure high turbulence levels and short mixing times. Precipitation was carried out with and without quenching, in order to highlight the possible influence of aggregation; to this purpose, the outlet of the mixer (8 mL containing equal volumes of acetone and water) was collected in a beaker containing 4 mL of water. Tests have been carried out in order to identify the best quenching volume ratio. When this is too small, it could be ineffective in stabilizing the system but when this is too large, it makes it impossible to use the sample for further characterization (unless extensive and therefore extremely time-consuming water evaporation is carried out). Four milliliters of water (corresponding to a 1:2 acetone–water final ratio in the mixture) was found to be a good trade-off, as quenching with larger volumes did not result in significantly different data, still resulting in reasonable final nanocapsule concentration.

The solubility of the copolymer for three water–acetone mixtures was studied. The investigated water volume fractions were 0.5, 0.66 (equivalent to 2/3), and 0.9, corresponding to the three conditions used in our experiments. In fact, samples without quenching result in mixtures of 0.5, whereas in quenched samples, the water is twice the acetone, resulting in 2/3. The last condition corresponds to a sample wherein the largest part of the acetone has been removed. These experiments were performed at 30°C.

In our laboratory set up, solvent solution and antisolvent were loaded into two different plastic syringes of 100 mL of volume and fed into the mixers by using a syringe pump (KDS200, KD Scientific, Holliston, MA, USA). The pump was calibrated in order to make sure that the imposed flow rate (FR) was actually delivered. Then, the solvent was removed by a rotating low-pressure evaporative device (Stuart® Rotary Evaporators). The possible azeotrope for the acetone–water mixture is in the acetone-rich region; therefore, complete removal of acetone is possible (as the starting point is an already water-rich solution). The effect of acetone removal on nanocapsules was quantified and found to be within the range of experimental uncertainty. Stability of the nanocapsule size after solvent removal was monitored by storing samples at 4°C for several weeks and measuring the nanocapsule size at regular time interval. No significant size changes were detected.

Four different CIJMs were used in this work. They all are similar but are characterized by different size of the inlet and outlet pipe and of the mixing chamber. A sketch is reported in Figure 1, whereas the detailed quotes are reported in Table 1. They are labeled in what follows as scale-down, CIJM-d1, scale-up (corresponding to three CIJMs exactly scaled-up by a geometric factor equal to two), and CIJM-d2 (corresponding to the same chamber size of CIJM-d1 but with bigger inlet pipe). The comparison of the results obtained with these four mixers allows to evidence scale-up and scale-down effects, as well as the effect of the chamber and inlet pipe size on the final size distribution.

Nanocapsules and nanospheres were characterized in terms of their size distribution (although reported data refer only to the mean size) and zeta potential and spherical shape was confirmed by Field Emission Scanning Electron Microscope (FESEM) pictures. The size of nanocapsules was determined by DLS (DLS, Zetasizer Nanoseries ZS90, Malvern Instrument, Worcestershire, UK) that measures accurately in the size range from 2 nm to 3 μm. Zetasizer Nanoseries ZS90 does not use a movable detector but uses classical fixed detection arrangement at 90° to the laser and the center of the cell area. In DLS measurements, the intensity size distribution is converted by using the Mie theory to a volume size distribution. In order to obtain the volume size distribution, it is necessary to provide the instrument the refractive index of the material (which does not significantly influence the final result of the measurement) and of the dispersant. Before measuring, the sample was diluted to 1:100 in order to reduce the solid concentration. In DLS, it is important to have a sample with appropriate particle concentration; in fact, it has not to be too concentrated because each single photon should be scattered only once before reaching the detector, but it has to be concentrated enough to result in sufficient statistics. The parameters which assure the quality of the measurements (i.e., polydispersion index, correlation function parameter) were controlled for

each single sample and measurements were repeated when the quality criteria were not reached. Each sample was measured three times and the average value is reported in the figures. Thus, in the following figure, *z*-average values are reported.

The surface charge of nanoparticles was inferred through zeta potential measurements in water, by the same instrument, after dilution (1:10). In zeta potential measurements, the instrument measures the electrophoretic mobility, which is the velocity of a particle in an electric field. The zeta potential is then calculated from the Henry equation that makes use of the Smoluchowski approximation, valid for particles in aqueous samples.

All the experiments were performed after dissolving the copolymer and the oil in the acetone. No stabilizing agent was added to the aqueous phase as the PEGylated polymer can act as a stabilizer due to its amphiphilic nature.

In order to investigate the interplay between mixing and nanocapsule formation, experiments were carried out in a wide FR range up to 120 mL/min for both solutions. Results from our previous work**17**show that under these conditions, the mixers work under different fluid dynamics regimes. In fact, the flow is highly turbulent only at the highest FRs (larger than 40 mL/min for the smallest mixers and larger than 90 mL/min for the biggest mixers) and is instead transitional for the lowest FRs. In all cases, however, the outlet stream is well mixed, as also at relatively low FRs, good mixing performances are generally obtained. The reason for investigating the performance of these devices also at low FRs, when the flow is not fully turbulent, is to verify the possibility of using mixing as an operating parameter to control the final nanocapsule size.

In these experiments, the acetone solution contained 6 mg/mL of copolymer and 8 μL/mL of oil (7.6 mg/mL), equivalent to an oil-to-copolymer mass ratio (MR) value of MR = 1.26. We performed the experiments both with and without quenching to understand the mechanism of nanocapsule formation and the main differences with respect to nanospheres. In same cases, experiments were repeated three times in order to quantify the experimental variability, reported together with the data in the form of error bars.

The effect of oil concentration on nanocapsule size was studied at four different oil concentrations: 0 (i.e., nanospheres), 4.8 μL/mL (4.56 mg/mL), 8 μL/mL (7.6 mg/mL), and 15 μL/mL (14.25 mg/mL) with 6 mg/mL of copolymer concentration. The respective oil-to-copolymer MR was 0.76, 1.26, and 2.37. These experiments were performed in all the CIJMs. Moreover, the same experiments were performed in the CIJM-d1, varying the copolymer concentration (10, 6, and 3.2 mg/mL). In this case, the oil concentration was kept constant at 8 μL/mL; in this way, the oil-to-copolymer MR was the same of the previous experiments (0.76, 1.26, and 2.37).

A further set of experiments, keeping constant the oil-to-copolymer mass ratio (MR), was also carried out. In this case, both copolymer and oil concentrations varied in order to check if it resulted in nanocapsules with similar size. The two MRs considered were 0.76 (with the following different concentrations: 4 mg/mL copolymer and 3.2 μL/mL oil, 6 mg/mL copolymer and 4.8 μL/mL oil, 10 mg/mL copolymer and 8 μL/mL oil) and 2.37 (3.2 mg/mL copolymer and 8 μL/mL oil, 6 mg/mL copolymer and 15 μL/mL oil). This set of experiments was carried out only in CIJM-d1 mixer.

Both the FR and the inlet diameter (d_{in}) of the mixer were varied in the experiments resulting in different mixing regimes inside the device. FR, velocity of the inlet jet (v_j), and d_{in} are related through the following relationship:

$$\pi \frac{d_{in}^2}{4} v_j = FR, \quad (1)$$

At the same FR, the fluid velocity is different in different mixers, resulting in different mixing efficiencies. According to Johnson and Prud'homme,**27** the overall mixing time (τ_{mix}) can be calculated as follows:

$$\tau_{mix} \propto v_j^{-3/2}, \quad (2)$$

when the flow is fully turbulent and, of course, different mixers are characterized by different residence times:

$$\tau_{res} = \frac{V_M}{FR} \quad (3)$$

where τ_{res} is the residence time and V_M is the volume of the mixer.

RESULTS AND DISCUSSION

Solubility tests revealed that the polymer residual concentration in the water–acetone mixture is significant when there is an equal amount of water and acetone and this amount slightly decreases when the water amount increases. A reduction in residual solubility is in fact detected when almost all the acetone (90%) is removed. Results are summarized in Table 2. This suggests that during acetone removal, additional polymer molecules can deposit on already formed nanocapsules and nanospheres. However, this amount does not significantly impact on the final particle size, as size measurements performed before and after removal (data not shown) highlighted very limited variations.

Nanocapsule formation was firstly investigated by comparing different mixers and different FRs (with and without quenching) and subsequently by comparing different initial compositions (copolymer and oil concentration). Results for the three CIJMs geometrically similar are reported in Figure 2. The figure shows the zeta potential and the mean particle size for nanocapsules prepared

with an acetone solution of 6 mg/mL of copolymer and 8 μL/mL of oil (resulting in MR = 1.26) at different FR values, with and without quenching.

Let us first highlight the effect of the quenching water; if nanocapsules are not quenched, their final mean size (after solvent evaporation) is significantly larger; this general behavior will be observed in all the cases investigated, and will be discussed as follows.

A common trend for all the mixers can be observed: increasing the FR, faster mixing is achieved, resulting in smaller particles. It is also interesting to observe that it is the same for both the quenched and the nonquenched particles. The data seem to evidence a point after which further increases in FR has little effect; this is expected by previous works in similar fields. The goal of using special intensive mixers (such as the ones used in this work) is to ensure that the mixing time is fast enough (in comparison with the particle formation time) so that the system can be considered homogeneous. It is not completely correct to specify a single break point, as in the range considered; in fact, the size is affected by fluid dynamics in a similar way, but this is true on a logarithmic scale. The effect of a variation of the inlet FR is strong at low FRs (generally below 20 mL/min), whereas it is very weak at higher FRs, generally larger than 40 mL/min. Results seem to show that mixing can also be used as an active parameter to control particle size. If one wants smaller particles, higher FRs (and faster mixing rates) should be used; on the contrary, if one wants bigger particles, smaller FRs (and slower mixing rates) should be used. This can be done until an effect of the wideness of the size distribution is detected. As simulations for a similar system show, in some cases there is a significant effect of mixing on particle size but a very limited one on polydispersity (especially when this is quantified as relative to the mean particle size). The combination of these two factors results in the possibility of playing with mixing only for the fine tuning of particle size, leaving almost unchanged relative polydispersity.

It must be said that at very low FR the uncertainty of the experimental data is relatively high, especially for the larger mixers, for which a lower reproducibility is observed; this may be a consequence of the fluid dynamic regime, as the inlet jets are laminar and thus the flow in the chamber is in the transitional region, with turbulence developing. In any case, it seems that the size increase that is observed, even when no quench is used, is similar in the whole range investigated, including the low FR region, thus confirming that the mixing performances of these devices are good also in the laminar regime.

In Figure 2, the performances of the three mixers are compared plotting the size of the nanocapsules obtained versus the inlet FR (the FR in each of the two inlets is considered), in order to evidence the influence of the size of the apparatus at constant throughput. The measured zeta potential is, as

average, between −30 and −45 mV, indicating that nanocapsules are stable from the electrochemical point of view. They reach lower values (−40 and −50 mV) if water dilution is carried out.

The scale-down mixer results in the smaller nanocapsules, probably due to the fact that it gives the best mixing conditions, at fixed FR. As scale-down mixer inlet jet diameter is 0.5 mm, the inlet stream can reach very high velocities, and as a consequence, high turbulent energy dissipation rates, and very short mixing times. But the inlet jet velocity is not the controlling variable, as shown in Figure 3; in fact, it can be noted that comparing the size obtained in the different mixers at the same inlet velocity, the conclusion is reversed, and the smallest nanocapsules are obtained in the scale-up mixer, whereas the scale-down mixer gives larger particles (and with higher energy costs). Only the quenched particle case is shown, but the behavior is similar (at least for the three-scaled mixers) for the nonquenched case. In these cases, the ratio between the inlet jet diameter and the chamber size is maintained constant, thus it is not possible to evidence which one of these geometrical variables eventually is more important, but it may be concluded that a larger size is surely favorable because it allows to increase throughput, reducing at the same time the final particle size (or eventually to obtain the same size at reduced jet velocity, and thus with lower energy input).

It is thus evident that the size of the apparatus plays a more complex role; if the Reynolds number is used to characterize the fluid dynamic conditions, and thus mixing, it is observed that the curves corresponding to the three mixers collapse onto a single one. Of course, Reynolds number can take into account only fluid dynamics similarity and only for geometrically similar devices, thus the behavior described above is observed only for the three-scaled mixers and for the same inlet concentrations of oil and polymer (that is for a fixed characteristic process time).

More complex to explain is the behavior of the CIJM-d2, which has the same chamber of the CIJM-d1, but larger inlet pipe diameters, equal to those of the scale-up device; in particular, significant differences are observed with and without quench. When nanocapsules are quenched, the size of the particles obtained, at a given FR, is approximately the same in the CIJM-d2 and in the scale-up mixer. It can be noted that in this case the inlet velocity is also the same, as the pipe diameter is equal (see also Fig. 3); this would suggest that the jet velocity is more relevant than the chamber size to determine mixing conditions. On the contrary, at a given jet velocity, smaller particles are obtained in the CIJM-d2 than in CIJM-d1; this might indicate that, for a given chamber volume, it is favorable to have a larger interaction zone of the two streams. It can be noted anyway that operating at the same jet velocity in the two considered mixers requires larger FRs in the one with larger pipe diameters (the CIJM-d2), and this leads to proportionally shorter residence times; thus, the smaller

size might be also a consequence of the reduced time for coalescence, and connected to a lower yield of the process.

If the outlet flow is not quenched, the behavior is different. At a given FR, the CIJM-d2 produces particles significantly larger than all the others, and in particular larger than the scale-up mixer; comparing the performances at a given inlet velocity, CIJM-d2 and CIJM-d1 produce nanocapsules of similar size. The comparison with the scale-up mixer evidences that in this case a larger chamber is favorable, as it allows to obtain smaller nanocapsules; as suggested by Johnson and Prud'homme,**27**what may be relevant is the ratio between the inlet pipe diameter and a characteristic chamber dimension and this value must not be too large to allow the mixing to be confined within the chamber. It is possible that in CIJM-d2, the particle formation process is not completed in the mixer, and this can explain the significant size increase observed in case of nonquenched nanocapsules; the CFD simulations carried out in a previous work for the same geometry confirm that the mixing process (at very low FRs) may be not complete.**18** This fact may be also responsible for the larger experimental uncertainty that is observed in the test carried out in the CIJM-d2.

The influence on the mean nanocapsule size of the inlet pipe diameter, for mixers with the same chamber volume, is shown in Figure 4; in this case, the data are plotted considering the inlet jet Reynolds number (for an inlet jet with average properties of the mixed liquid streams). It can be noted that in case of quenched nanocapsules, a unique curve is obtained (and as discussed before, this is the same curve valid for all the mixers in these concentration conditions), whereas for nonquenched ones, larger sizes are obtained in the CIJM-d2, as discussed before. Figure 4 allows also to compare the experimental uncertainty in the case of quenched and nonquenched processes; in the latter case, it is significantly higher. Zeta potential measurements (not shown) result in values slightly lower than −30 mV.

These results show the feasibility of CIJMs for the production of nanocapsules and prove that fast mixing is needed in order to control nanocapsules size and in order to guarantee high reproducibility. Better mixing conditions allow the formation of smaller oily drops and a better coverage by the copolymer, resulting in smaller particles. Moreover, results show that quenching is an important factor and cannot be avoided if nanocapsules with controlled characteristics are desired. It may be also concluded that the process can be scaled using the Reynolds number, at least for geometrically similar devices; the relative size of inlet pipes and chamber has shown to affect the process, but its influence on final nanocapsule size is complex, and cannot be taken into account with a simple relationship, such as that proposed for the mixing time in literature.**27** Also the influence of the mixing time will require further work to be quantified in the case of this specific

394 application. In fact, the results obtained confirm that process kinetics and mixing interact and when
395 reducing the mixing time, smaller particles are obtained. However, modifications of the mixer size
396 and geometry cannot be taken into account simply by the variation in the mixing time estimated in
397 the different mixing devices, even for the same inlet polymer and oil concentrations. In fact, using
398 the mixing times estimated by CFD simulations**18**for the different mixers to correlate the particle
399 size obtained, it is not possible to obtain a unique curve for the runs obtained in different mixers.
400 The effect of oil concentration on nanocapsule formation was also investigated. At a constant
401 copolymer concentration of 6 mg/mL, the oil concentration was varied between zero (resulting in
402 nanospheres) and a maximum value. Data are collected in Figure 5, where the results obtained for
403 four different oil-to-copolymer MRs are reported for each mixer; the data are plotted versus the
404 Reynolds number, on the basis of the results discussed in the previous parts of this work, and as the
405 experiments were carried out in the same flow rate range for the different mixers, obviously the
406 extension of the jet Reynolds number range investigated is different. The results confirm that for
407 every set of concentrations, a single curve is obtained for the different scaled mixers (in fact, the
408 approximation curve drawn in the different graphs of the figure is this common line), whereas a
409 behavior similar to that discussed before is observed for the CIJM-d2. These conclusions are
410 generally valid also for other polymer concentrations, but as it will be shown in the following, for
411 very low polymer concentrations, the formation of nanocapsules may be difficult.
412 As a general trend, it is possible to state that decreasing the oil-to-copolymer MR, the mean particle
413 size decreases. That can be due to the fact that when the oil-to-copolymer MR increases, there is not
414 enough copolymer to cover a larger surface area, resulting in bigger nanocapsules.
415 Each experiment at a given oil-to-copolymer MR was repeated with and without quenching water.
416 Quenching reduces the final nanocapsule size, but the effect is stronger at higher ratios, where there
417 is a lower amount of copolymer. As already mentioned, the operation of quenching allows to stop
418 nanocapsule evolution and freeze them as they are immediately after exiting the CIJM. In fact,
419 quenching dilutes the residual polymer concentration and the particulate system decreasing the
420 probability of nanocapsule collision and further growth. If we compare the results at different oil-to-
421 copolymer MRs, it is clear that the size increase is more relevant at high MR values, where there is
422 less copolymer to cover the oily drops. As a matter of fact, the results obtained at MR = 0.76
423 present a very small difference with or without quenching. This suggests that the copolymer coating
424 has an important role in stabilizing the suspensions and avoiding nanocapsule aggregation and
425 coalescence.
426 In Figure 5 also nanospheres produced under similar operating conditions are shown for
427 comparison; the size is always much smaller than that obtained in nanocapsules, which is mainly

428 determined by the size of the oil drops formed, suggesting that size increase can take place for
429 further aggregation of copolymer molecules from the solution and not for the collision of the
430 nanospheres.
431 In comparison to nanospheres (MR = 0), where there is no oil inside, in nanocapsule, the energy
432 barrier that has to be overcome due to repulsion forces in case of aggregation seems to be lower due
433 to the presence of the oil. Thus, the stability of the nanocapsule suspension could be related with the
434 thickness of the copolymer wall formed. This will surely decrease if the oil-to-copolymer MR is
435 increased and in the case considered is the largest at MR = 0.76. Moreover, we can assume that
436 good mixing allows more copolymer to be available for covering oily drops.
437 As noted in Figure 2, particle size does not significantly change when working with FR values
438 greater than 40 mL/min. That probably happens because the system reaches good mixing
439 conditions, which guarantee small particle size. Comparison with the data shown in
440 Figure 5 highlights an additional element. If we consider particle size obtained at Reynolds numbers
441 greater than 1000 (i.e., high mixing efficiency), the differences among the mixers are very small for
442 each MR investigated. In fact, the variation of particle size at each MR is smaller than 40 nm,
443 suggesting that the effect of the mixer geometry is very low when the highest mixing efficiency is
444 reached. Moreover, results are very reproducible at high mixing efficiency, on the contrary to what
445 happens under laminar conditions, where the data from different geometries are more scattered.
446 In Figure 6, zeta potential is shown as a function of the size for nanocapsules obtained with
447 different mixers, the FRs and oil-to-copolymer ratios. As it is possible to see no significant
448 differences are detectable depending on the mixers used, showing that both nanocapsules and
449 nanospheres present the same superficial properties independently on the mixer used, small
450 differences seem to exist between nanocapsules and nanospheres, but no significant differences are
451 noted among nanocapsules obtained at different MR. The fact that the presence of the oil does not
452 impact the final zeta potential value of nanocapsules could be interpreted as a proof of the fact that
453 the oil stays inside the copolymer shell. This hypothesis is supported by preliminary experimental
454 evidences obtained with X-ray photoelectron spectroscopy**28** and will be reported in future
455 communications.
456 As previously mentioned, the copolymer concentration was also varied, keeping constant the oil
457 concentration. Experiments were performed only in CIJM-d1 with and without quenching and all
458 the previous trends were confirmed, as shown in Figure 7 where the data are plotted versus
459 Reynolds as in previous cases. It may be noted that at low polymer concentration, the size of the
460 nanocapsules measured becomes extremely large, and it is evident that the situation must be
461 different from the other cases, where a proportional variation of the polymer had a relatively small

effect. Probably, under these conditions, the polymer quantity available for the formation of the copolymer shell is too small, and the forming nanocapsules collapse; further work will be necessary to investigate what happens under these limiting conditions.

Figure 8 shows results for nanocapsules obtained with CIJM-d1 for different initial oil and copolymer concentrations, but at the same relative MR to investigate the role of the total concentration of both copolymer and oil.

Results confirm that the copolymer concentration can play also an important role in the final nanocapsule size, as it stabilizes oily drops and prevent further coalescence. In particular, they clearly show that at MR lower than one, the total concentration of polymer and oil is not important, but it is their MR that determines the final size, indicating that the copolymer is able to block oily drops growth by surrounding them; at higher MRs, results depend on the polymer concentration. As already mentioned, working at high mixing intensity (Reynolds numbers greater than 1000) the mean particle size is, on average, between 170 and 280 nm, depending on the mixer and on the MR. The only data point which does not fall within this range was obtained at MR 2.37 with a copolymer concentration of 3.2 mg/mL and oil concentration of 8 μL/mL. This data set shows a mean particle size drastically larger than that for samples obtained under similar operating conditions, even in case of quench; the relative increase observed for nonquenched particles, then, is very relevant. Moreover, the solubility data already discussed show that there is a copolymer amount remaining in the solution (0.2 g/L in acetone–water mixture at 90% of water) that has to be subtracted from the initial copolymer concentration to give the effective available copolymer amount. This is naturally more important at low initial copolymer concentrations, as in the case of 3.2 mg/mL.

To conclude, this second data set shows that increasing the copolymer amount, nanocapsule size decreases and probably copolymer wall thickness increases. Quenching is useful in stabilizing the system, preventing further aggregation especially when the copolymer amount is lower (and probably the copolymer wall is thinner), but below a certain polymer concentration, nanocapsules of controlled size cannot be obtained; the limit conditions, that probably depend on residual polymer solubility in the liquid mixture, and on process yields, require further investigation.

CONCLUSIONS

We synthesized a PEGylated cyanoacrylate amphiphilic copolymer, in order to prepare nanocapsules for pharmaceutical applications. PEGylated copolymers are very useful in the pharmaceutical field as they increase the blood lifetime of particulate carriers. At the same time,

they are advantageous as they act as stabilizers, allowing to work without additional stabilizing agents, thus reducing the costs and avoiding possible toxicity problems.

Nanocapsules were prepared for the first time using CIJMs. These devices provide good mixing and were already used for obtaining nanoparticles of different materials. The mechanisms involved in nanocapsule formation inside these devices are still not completely clear, as nanocapsules are a complex system with more variables involved. The influence of mixer geometry on nanocapsule formation needs more investigation, especially to understand how the overall mixing time affects the final nanocapsule size and copolymer distributions.

The results reported in this work demonstrate that CIJMs can be successfully used in nanocapsule production and represent possibility route for their continuous production. Different types of nanoparticles are now reaching the clinical trial level; therefore, a continuous route for producing them with reproducible characteristics is highly desirable.

Further investigations on the pharmaceutical properties of nanoparticles produced by this way are required, in order to give a complete evaluation of the product and of the system together with the limiting operating conditions that allow to obtain stable nanocapsules.

REFERENCES

1)Ammoury N, Fessi H, Devissaguet JP, Puisieux F, Benita S. 1990. In vitro release kinetic pattern of indomethacin from poly(d,l-Lactide) nanocapsules. J Pharm Sci 79:763–767.

2) Stella B, Arpicco S, Rocco F, Marsaud V, Renoir JM, Cattel L, Couvreur P. 2007. Encapsulation of gemcitabine lipophilic derivatives into polycyanoacrylate nanospheres and nanocapsules. Int J Pharm 344:71–77.

3) Vauthier C, Labarre D, Ponchel G. 2007. Design aspects of poly(alkylcyanoacrylate) nanoparticles for drug delivery. J Drug Target 15:641–663.

4) Peracchia MT, Gref R, Minamitake Y, Domb A, Lotan N, Langer R. 1997. PEG-coated nanospheres from amphiphilic diblock and multiblock copolymers: Investigation of their drug encapsulation and release characteristics. J Control Release 46:223–231.

5) Bouchemal K, Briancon S, Fessi H, Chevalier Y, Bonnet I, Perrier E. 2006. Simultaneous emulsification and interfacial polycondensation for the preparation of colloidal suspensions of nanocapsules. Mater Sci Eng C 26:472–480.

6) Pitaksuteepong T, Davies NM, Tucker IG, Rades T. 2002. Factors influencing the entrapment of hydrophilic compounds in nanocapsules prepared by interfacial polymerisation of water-in-oil microemulsions. Eur J Pharm Biopharm 53:335–342.

7) Peracchia MT, Vauthier C, Desmaele D, Gulik A, Dedieu JC, Demoy M, d'Angelo J, Couvreur P. 1998. Pegylated nanoparticles from a novel methoxypolyethylene glycol cyanoacrylate hexadecyl cyanoacrylate amphiphilic copolymer. Pharm Res 15:550–556.

8) Moinard-Checot D, Chevalier Y, Briancon S, Beney L, Fessi H. 2008. Mechanism of nanocapsules formation by the emulsion-diffusion process. J Colloid Interface Sci 317:458–468.

9) Garti N. 1997. Double emulsions—Scope, limitations and new achievements. Colloids Surf A-Physicochemical Eng Aspects 123:233–246.

10) Mora-Huertas CE, Fessi H, Elaissari A. 2010. Polymer-based nanocapsules for drug delivery. Int J Pharm 385:113–142.

539 11) Marchisio DL, Rivautella L, Barresi AA. 2006. Design and scale-up of chemical reactors for
540 nanoparticle precipitation. AIChE J 52:1877–1887.

541 12) Gavi E, Marchisio DL, Barresi AA. 2008. On the importance of mixing for the production of
542 nanoparticles. J Dispersion Sci Technol 29:548–554.

543 13) Gavi E, Marchisio DL, Barresi AA, Olsen MG, Fox RO. 2010. Turbulent precipitation in
544 micromixers: CFD simulation and flow field validation. Chem Eng Res Des 88:1182–1193.

545 14) Lince F, Marchisio DL, Barresi AA. 2008. Strategies to control the particle size distribution of
546 poly-ε-caprolactone nanoparticles for pharmaceutical applications. J Colloid Interface Sci
547 322:505–515.

548 15) Lince F, Marchisio DL, Barresi AA. 2009. Smart mixers and reactors for the production of
549 pharmaceutical nanoparticles: Proof of concept. Chem Eng Res Des 87:543–549.

550 16) Gavi E, Rivautella L, Marchisio DL, Vanni M, Barresi AA, Baldi G. 2007. CFD modelling of
551 nano-particle precipitation in confined impinging jet reactors. Chem Eng Res Des 85:735–
552 744.

553 17) Lince F, Bolognesi S, Marchisio DL, Stella B, Dosio F, Barresi AA, Cattel L. 2010. Preparation
554 of poly(MePEGCA-co-HDCA) nanoparticles with confined impinging jets reactor:
555 Experimental and modelling study. J Pharm Sci 100:2391–2405.

556 18) Lince F, Marchisio DL, Barresi, AA. 2011. A comparative study for nanoparticle production
557 with passive mixers via solvent-displacement: Use of CFD models for optimization and
558 design, Chem Eng Process 50:356–368.

559 19) Alvarez-Roman R, Barre G, Guy RH, Fessi H. 2001. Biodegradable polymer nanocapsules
560 containing a sunscreen agent: Preparation and photoprotection. Eur J Pharm Biopharm
561 52:191–195.

562 20) Zambrano-Zaragoza ML, Mercado-Silva E, Gutiérrez-Cortez E, Castaño-Tostado E, Quintanar-
563 Guerrero D. 2011. Optimization of nanocapsules preparation by the emulsion–diffusion
564 method for food applications. Food Sci Technol 44:1362–1368.

565 21) Lince F, Bolognesi S, Stella B, Marchisio DL, Dosio F. 2011. Preparation of polymer
566 nanoparticles loaded with doxorubicin for controlled drug delivery. Chem Eng Res Des
567 89:2410–2419.

568 22) Horn D, Rieger J. 2001. Organic nanoparticles in the aqueous phase—Theory, experiment, and
569 use. Angew Chem Int Ed Engl 40:4330–4361.

570 23) Johnson BK, Prud'homme RK. 2003. Flash NanoPrecipitation of organic actives and block
571 copolymers using a confined impinging jets mixer. Aust J Chem 56:1021–1024.

572 24) Fessi H, Puisieux F, Devissaguet JPh, Ammoury N, Benita S. 1989. Nanocapsule formation by
573 interfacial deposition following solvent-displacement. Int J Pharm 55:R1–R4.

574 25) Quintanar-Guerrero D, Allemann E, Fessi H, Doelker E. 1998. Preparation techniques and
575 mechanisms of formation of biodegradable nanoparticles from preformed polymers. Drug Dev
576 Ind Pharm 24:1113–1128.

577 26) Peracchia MT, Desmaele D, Couvreur P, d'Angelo J. 1997. Synthesis of a novel poly(MePEG
578 cyanoacrylate-co-alkyl cyanoacrylate) amphiphilic copolymer for nanoparticle technology.
579 Macromolecules 30:846–851.

580 27) Johnson BK, Prud'homme RK. 2003. Chemical processing and micromixing in confined
581 impinging jets. AIChE J 49:2264–2282.

582 28) Valente I, Celasco E, Marchisio DL, Barresi AA. 2011. Nanoprecipitation in confined
583 impinging jets mixers: Production and characterization of pegylated nanoparticles for
584 pharmaceutical use. Proceedings of 18th International Symposium on Industrial
585 Crystallization; September 13–16, 2011; Zurich, Switzerland, 172–173.

586

Mixer	d_{in} (mm)	d_{out} (mm)	D_c (mm)	Volume (mm^3)
Scale-down	0.5	1	2.4	22.5
CIJM-d1	1	2	4.8	180.3
Scale-up	2	4	9.8	1288.3
CIJM-d2	2	2	4.8	180.3

Table 1. Geometrical details of the CIJMs used for the experiments.

Water Volume Fraction	0.5	0.66	0.9
g/L	0.45	0.4	0.243

Table 2. Polymer Solubility at Different Composition of the Water–Acetone Mixture

595

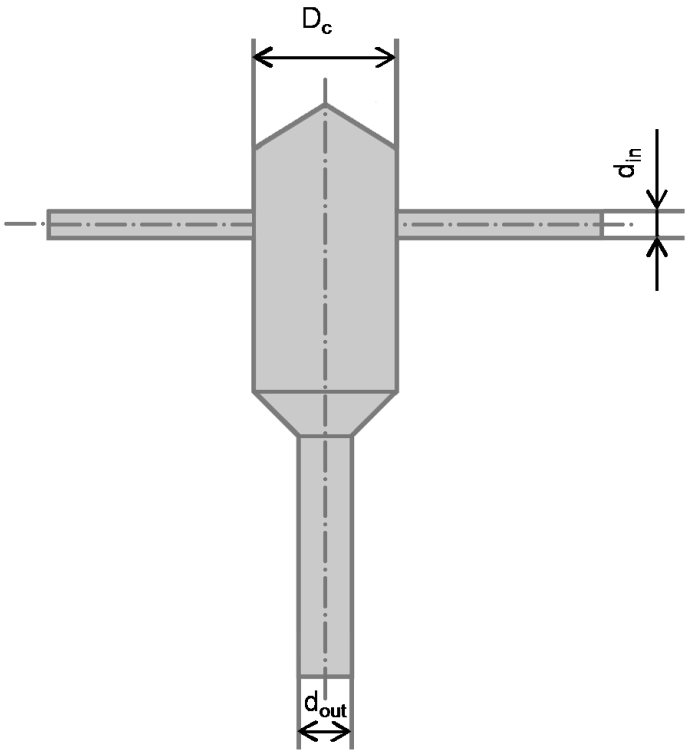

596

597 **Figure 1. Sketch of the CIJMs used in this work.**

598

599

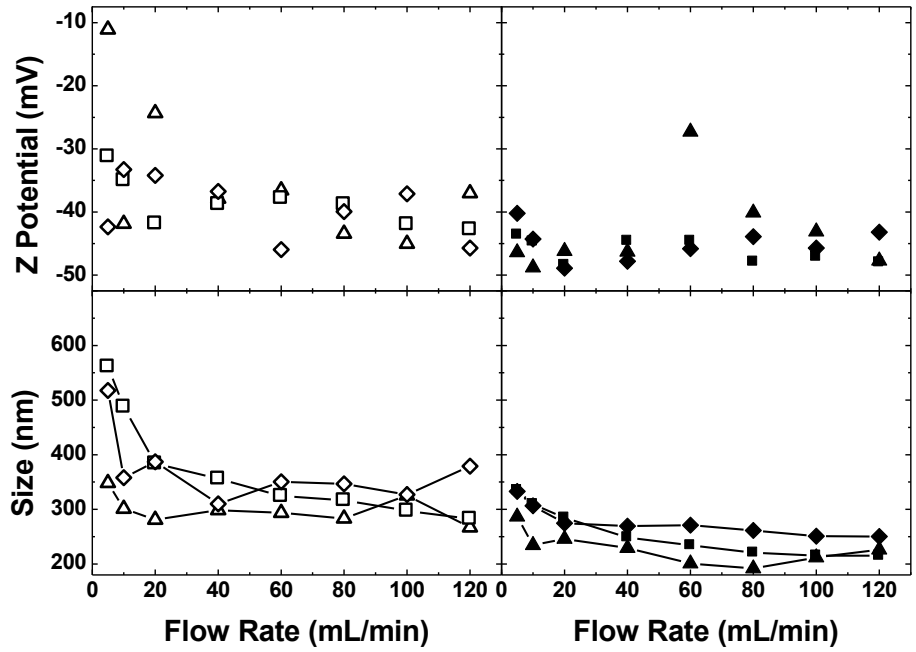

600

601 **Figure 2. Mean particle size (bottom) and zeta potential (top) versus the flow rate for nanocapsules obtained**
602 **without quenching water (left, open symbols) and with quenching water (right, filled symbols) for different**
603 **mixers: scale down (△,▲),CIJM-d1 (□,■) and scale up (◇,◆).Experiments at constant polymer (6 mg/mL)**
604 **and oil (8 µL/mL) concentration (MR = 1.26).**

605

606

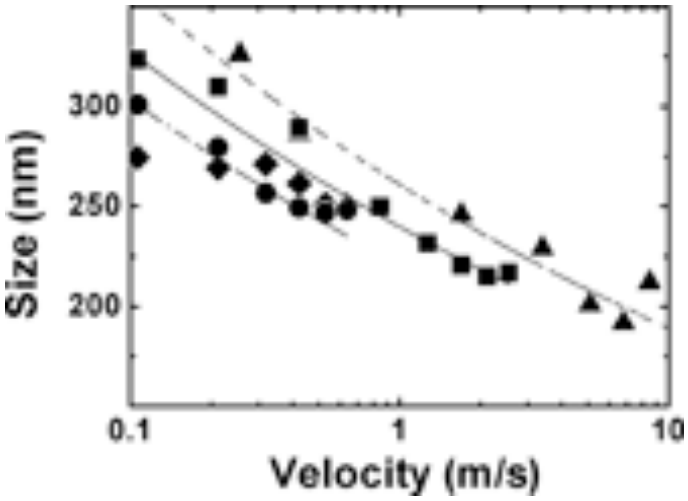

607

608 **Figure 3. Mean particle size versus the inlet stream velocity for nanocapsules obtained with different CIJMs:**
609 **scale-down mixer (▲), CIJM-d1 mixer (▪), scale-up mixer (♦), and CIJM-d2 mixer (•). Experiments at constant**
610 **polymer (6 mg/mL) and oil (8 µL/mL) concentration (MR = 1.26).**

611

612

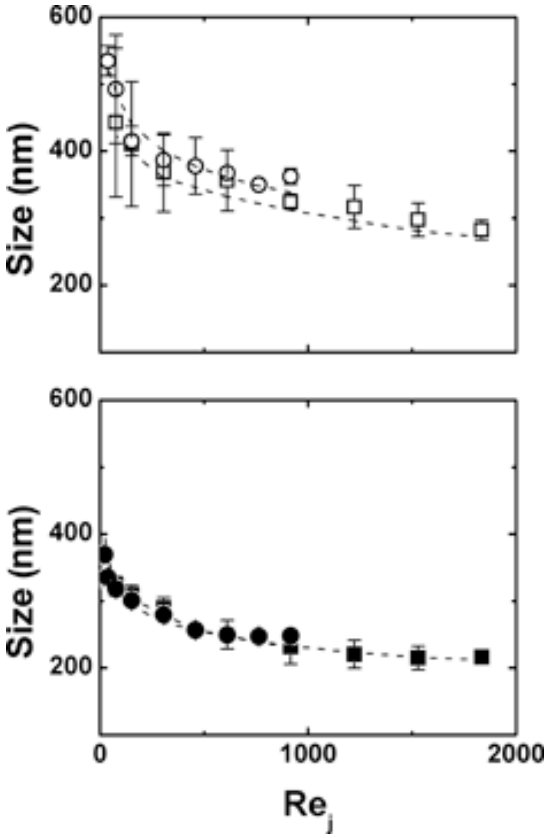

Figure 4. Mean particle size versus the jet Reynolds number for nanocapsules obtained without quenching water (top, open symbols) and with quenching water (bottom, filled symbols) for CIJMs characterized by different inlet pipes and same mixing chamber: CIJM-d1 (□,▪), CIJM-d2 (○,•). Experiments at constant polymer (6 mg/mL) and oil (8 µL/mL) concentration (MR = 1.26).

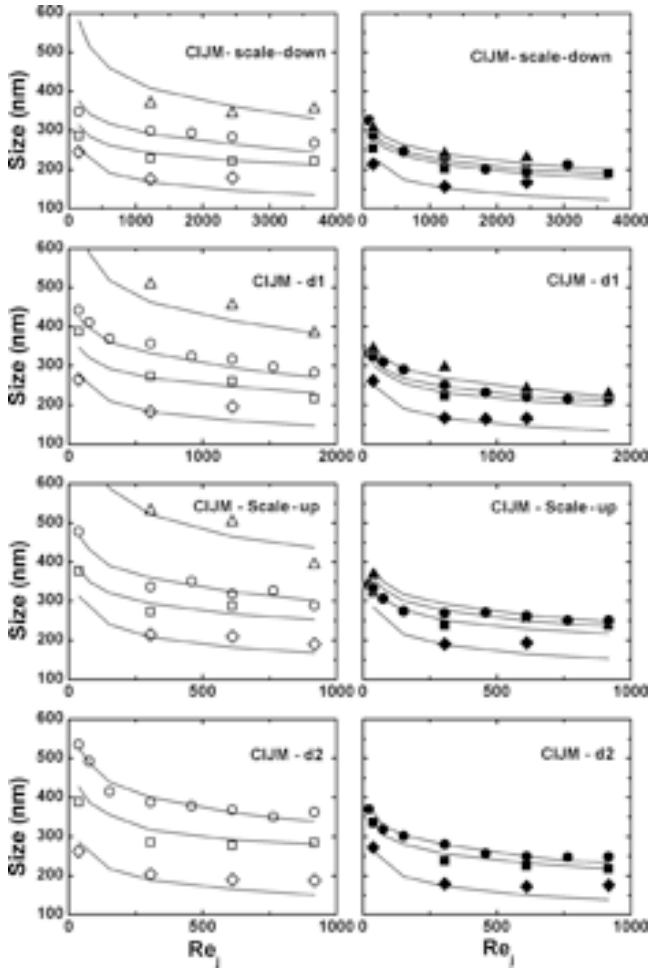

Figure 5. Mean particle size versus the jet Reynolds number for nanocapsules and nanospheres obtained at four different oil-to-copolymer mass ratios, MR = 0 (◇,♦), MR = 0.76 (□,▪), MR = 1.26 (○,•), and MR = 2.37 (▵,▲) without quenching (left, open symbols) and with quenching (right, filled symbols) for (from top to bottom) scale-down, CIJM-d1, scale-up, and CIJM-d2. Constant polymer concentration (6 mg/mL).

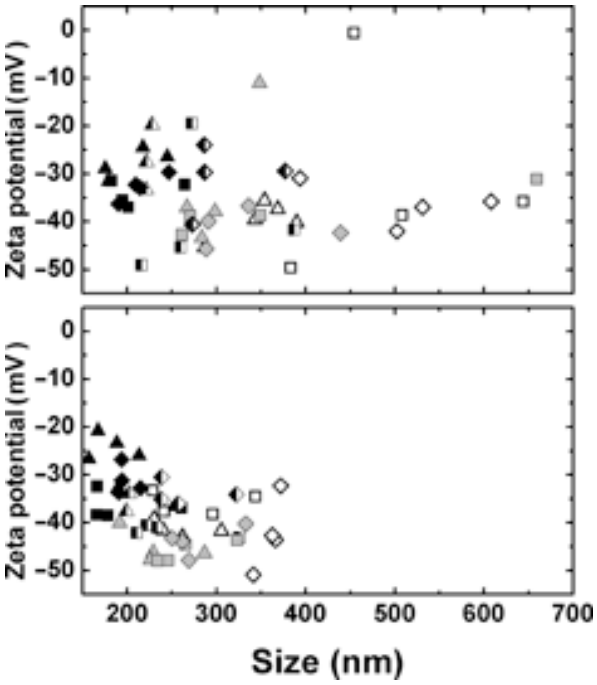

629

630 **Figure 6. Zeta potential as a function of particle size obtained with different mixers: scale-down (triangle),**
631 **CIJM-d1 (square), and scale-up (rhomb). Top graph: particles without quenching. Bottom graph: particles with**
632 **quenching. Both nanospheres and nanocapsules are present: nanospheres (black), nanocapsules at MR = 0.76**
633 **(half black), nanocapsules at MR = 1.26 (light gray), and nanocapsules at MR = 2.37 (white).**

634

635

636

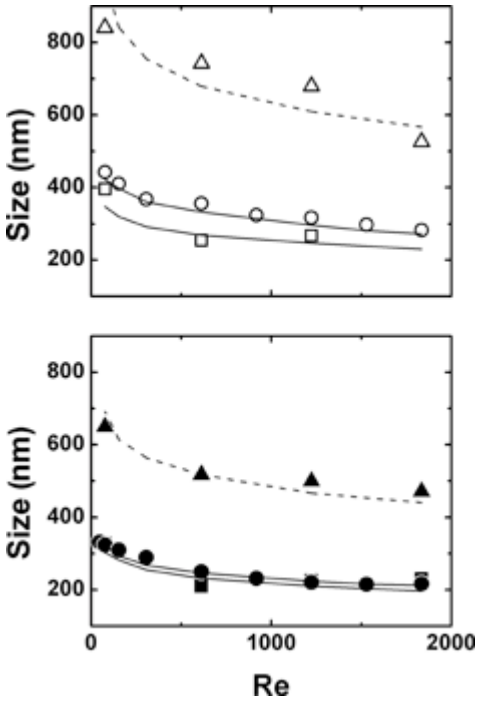

Figure 7. Mean particle size versus the jet Reynolds number for nanocapsules obtained at constant oil concentration (8 µL/mL) and at copolymer concentration of 10 mg/mL (MR = 0.76, □,▪), 6 mg/mL (MR = 1.26, ○,•), and 3.2 mg/mL (MR = 2.37, ▵,▲) in CIJM-d1 without quenching (open symbols) and with quenching (filled symbols).

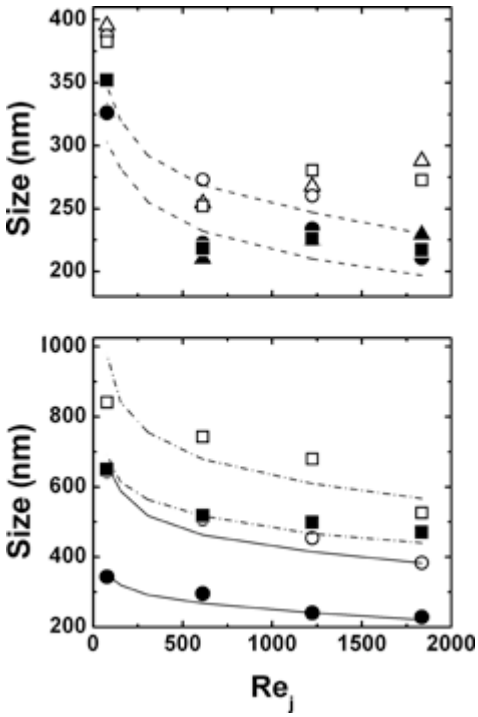

Figure 8. Mean particle size versus the jet Reynolds number for nanocapsules obtained with CIJM-d1 without quenching (open symbol) and with quenching (filled symbol) at two different constant oil-to-copolymer mass ratio for different copolymer and oil concentrations; upper graph: MR = 0.76 with 4 mg/mL copolymer and 3.2 µL/mL oil (□,▪), 6 mg/mL copolymer and 4.8 µL/mL oil (○,•), 10 mg/mL copolymer, and 8 µL/mL oil (□,□); lower graph: MR = 2.37 with 3.2 mg/mL copolymer and 8 µL/mL oil (□,▪,–––), 6 mg/mL copolymer, and 15 µL/mL oil (○,•, ——).